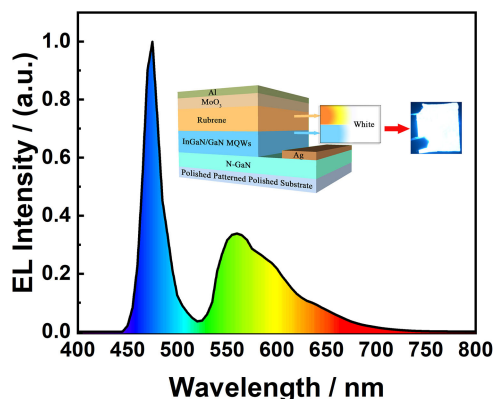🔓 **Open Access**

Electrically Injected Hybrid Organic/Inorganic III-Nitride White Light-Emitting Diodes Based on Rubrene/(InGaN/GaN) Multiple-Quantum-Wells P-N Junction

Danbei Wang
Bin Liu
Hongmei Zhang
Hong Zhao
Tao Tao
Zili Xie
Rong Zhang
Youdou Zheng

Electrically Injected Hybrid Organic/Inorganic III-Nitride White Light-Emitting Diodes Based on Rubrene/(InGaN/GaN) Multiple-Quantum-Wells P-N Junction

Danbei Wang,[1] **Bin Liu,**[1] **Hongmei Zhang,**[2] **Hong Zhao,**[1] **Tao Tao,**[1] **Zili Xie,**[1] **Rong Zhang,**[1,3] **and Youdou Zheng**[1]

[1]Jiangsu Provincial Key Laboratory of Advanced Photonic and Electronic Materials, School of Electronic Science and Engineering, Nanjing University, Nanjing 210093, China
[2]Institute of Advanced Materials, Nanjing University of Posts and Telecommunications, Nanjing 210023, China
[3]Xiamen University, Xiamen 361005, China

Abstract: It is known that the commercialized white light-emitting diodes (WLEDs) depend on phosphor conversion, which is limited by the unbalanced carrier injection in multiple quantum wells (MQWs) and low down-conversion efficiency. To solve these problems, hybrid organic/inorganic III-nitride WLEDs were designed and fabricated based on Rubrene/(InGaN/GaN) MQWs p-n junction. In such new structure, Rubrene can act as yellow–red emitter and play an important role in hole transport layer owing to its high carrier mobility. By optimizing the hybrid LED structure, the charge balance and recombination zone in radiative region were significantly improved. In this work, the optimal hybrid WLED with color coordinates of (0.31, 0.33) shows a maximum current efficiency of 15.22 cd/A with excellent long lifetime stability. The hybrid WLEDs based on organic/inorganic p-n junction were demonstrated with a good performance, which provides an attractive route to achieve high performance phosphor-free WLED sources for microdisplay or large-area WLED applications.

Index Terms: III-nitrides, organic materials, p-n junction, light emitting diodes, white electroluminescence, hole transport layer, exciton recombination.

1. Introduction

Over the last decades, tremendous developments in the field of white light emitting diodes (WLEDs) based on III-nitride semiconductors have been achieved, leading to the solid-state lighting revolution

and massive energy savings [1]–[3]. The current mainstream and commercialized WLEDs still rely on light-conversion technique, where yellow phosphor partially converting blue light emitting from a blue-emitting LED into yellow emission yielding white lighting. However, many negative effects need to be settled, including self-absorption, degradation, quenching of the phosphors and low energy transfer from the blue emission to the phosphor, which cause low luminous efficiency [4], [5]. Especially, the excess electrons overflow through the MQWs without recombination, leading to a low output efficacy and efficiency of light conversion [6]. To settle these problems, many efforts have been done to rebalance the current flow and develop efficient phosphor-free white LEDs [7]–[9].

Recently, the hybrid organic/inorganic technique has attracted increasing attentions as a promising platform for high performance WLED. Organic semiconductor materials have excellent optical property over the entire visible region [10], [11]. Compared with GaN-based LED, organic semiconductor materials also have better hole transport and/or electron blocking properties [12], [13]. Several other potential merits including simple fabrication process, low cost and the combination the complementary advantages of the two major semiconductor material groups, makes the combination of organic/inorganic system one of the most promising way towards high performance [14], [15]. It is apparent that the potential for organic materials as the emitting layer together with inorganic MQWs or as viable alternatives to conventional p-type inorganic semiconductor in the hybrid organic/inorganic LED. Moreover, the cohesive forces between organic molecules are weaker Van der Waals. As a consequence, organic materials can be deposited onto inorganic semiconductor without strain [16], [17]. Up to now, a number of researches on hybrid organic/inorganic III-nitride LEDs have been reported [14], [18], [19]. The optoelectronic characteristics of hybrid organic/inorganic devices are similar to those pure inorganic LEDs obtained by complicated processed. However, it remains a challenge to realize efficient electrically driven white light emission from single chip with both organic and inorganic active layers.

In this paper, electrically driven high-performance hybrid organic/inorganic white LEDs were designed and achieved based on Rubrene/(InGaN/GaN) MQWs p-n junction. By optimizing device structure, the hybrid organic/inorganic WLEDs with 75-nm-thick Rubrene exhibit the best device performance. Pure white emission with color coordinates of (0.31, 0.33) and a maximum current efficacy of 15.22 cd/A was achieved. To better understand the carrier transport and radiation mechanism of across the Rubrene/(InGaN/GaN) MQWs p-n junction in the hybrid WLED, ultraviolet-visible (UV-VIS), electroluminescence (EL), current-voltage (I-V) characteristics and carrier dynamics were systematic studied.

2. Experimental Details

2.1. MOCVD Growth of InGaN/GaN MQWs Structure

The hybrid organic/inorganic III-Nitride p-n heterojunction WLEDs were fabricated from InGaN/GaN MQWs epitaxial wafers grown by metal organic chemical vapor deposition (MOCVD) on c-plane patterned sapphire (0001) substrates. The epitaxy comprised a 2 μm undoped GaN buffer, 3 μm n-type GaN layer (silane doped, n$\sim$10^{19}/cm^3), and 10 periods of In$_{0.2}$Ga$_{0.8}$N/GaN MQWs, where the thicknesses of quantum wells and barriers were approximately 3 and 12 nm, respectively. The growth details can be referred in [20].

2.2. Organic Materials and Device Preparation

In hybrid structure, 5,6,11,12-Tetraphenylna-phthacene (Rubrene) and molybdenum oxide (MoO$_3$) serve as hole-transporting yellow-red active layer and hole injection layer, respectively. Rubrene has been widely used as yellow-red emitter or hole transport layer in organic optoelectronic devices due to its high emission efficiency, long exciton diffusion length and superior carrier mobility (up to 40 cm^2/Vs) [21]–[23]. Both materials purchased from Jilin OLED Material Tech Co. Ltd and used as received without further purification.
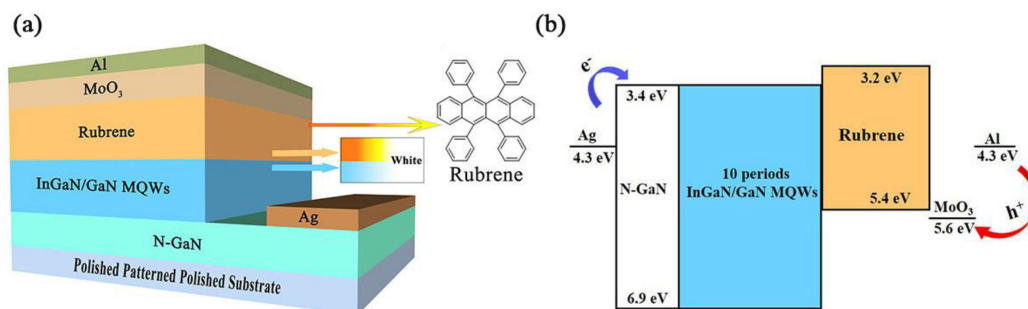
Fig. 1. (a) Schematic of the hybrid organic/inorganic III-Nitride WLED based on Rubrene/ (InGaN/GaN) MQWs p-n junction; (b) energy diagram of the resulting hybrid device.

Prior to usage, the above MOCVD-grown InGaN/GaN MQWs epitaxial layers were solvent-cleaned with successive treatments with detergent, de-ionized water, acetone and isopropyl alcohol in an ultrasonicator (Shumei KQ300DE). Each step was carried out for 10 min. After being blown dry with nitrogen gas, the cleaned wafers were treated with UV-ozone (UVO cleaner 42–220, Jelight Company Inc.) for 15 min for further clean as well as increasing the adsorptivity of the subsequent organic materials onto InGaN/GaN MQWs epitaxial layers. Then these wafers were fixed to the sample holder and transferred into the vacuum evaporation system (3×10^{-4} Pa). Rubrene, MoO_3, Al and Ag were all thermally evaporated onto InGaN/GaN MQWs epitaxial wafers. The deposition rates of Rubrene, MoO_3, Ag, Al were 1 Å/s, 0.2 Å/s, 3 Å/s and 5 Å/s, respectively. The evaporation rates were monitored by a quartz oscillator system and the film thickness was calibrated by a surface profiler (SQC-310, INFICON). The active area of each one is 16 mm^2.

2.3. Device Characterizations

The current-voltage-brightness characteristics were acquired by a system consisting of a Keithley source measurement unit (Keithley 2400 and Keithley, 2000) and a calibrated silicon photodiode. The EL spectra were measured by a Spectra-scan PR655 spectrophotometer. The absorption spectra of Rubrene was taken on a lambda 35 PerkinElmer UV-VIS spectrophotometer. The photoluminescence (PL) spectra of Rubrene film, InGaN/GaN MQWs and Rubrene(100 nm)/(InGaN/GaN) MQWs hybrid structure were measured using a 375 nm diode laser as an excitation source. Furthermore, the time-resolved PL (TRPL) measurements were collected by a time-correlated single-photon counting system (TCSPC) with a time resolution of 250 ps. The peak emission from the MQWs was selected using a Horiba Jobin Yvon iHR320 monochromator. All the characterizations presented were carried out in the ambient without encapsulation.

3. Results and Discussions

Fig. 1(a) illustrates the structure of the hybrid organic/inorganic III-nitride WLED based on Rubrene/(InGaN/GaN) MQWs heterojunction. The corresponding energy level diagram is shown in Fig. 1(b). It is worth noting that lowest unoccupied molecular orbital (LUMO) and highest occupied molecular orbital (HOMO) energy difference of Rubrene is 2.2 eV, which is close to the bandgap of the InGaN/GaN MQWs (2.6 eV determined by photoluminescence measurement at room temperature). Thus, injected charge carriers can be efficiently transported across the Rubrene/(InGaN/GaN) MQWs p-n junction [24]. As design, Rubrene layer was also employed as hole-transporting yellow-red active layer in this work.

To rebalance the current flow of across the Rubrene/(InGaN/GaN) MQWs p-n junction in this hybrid organic/inorganic III-nitride WLEDs, the thickness of Rubrene need to be optimized. In this work, the device structure is Ag (50 nm)/N-GaN/(InGaN/GaN) MQWs/Rubrene (X nm)/MoO_3 (5 nm)/Al (70 nm), where X is 25, 50, 75, 100 nm, respectively. The electroluminescence (EL) performances
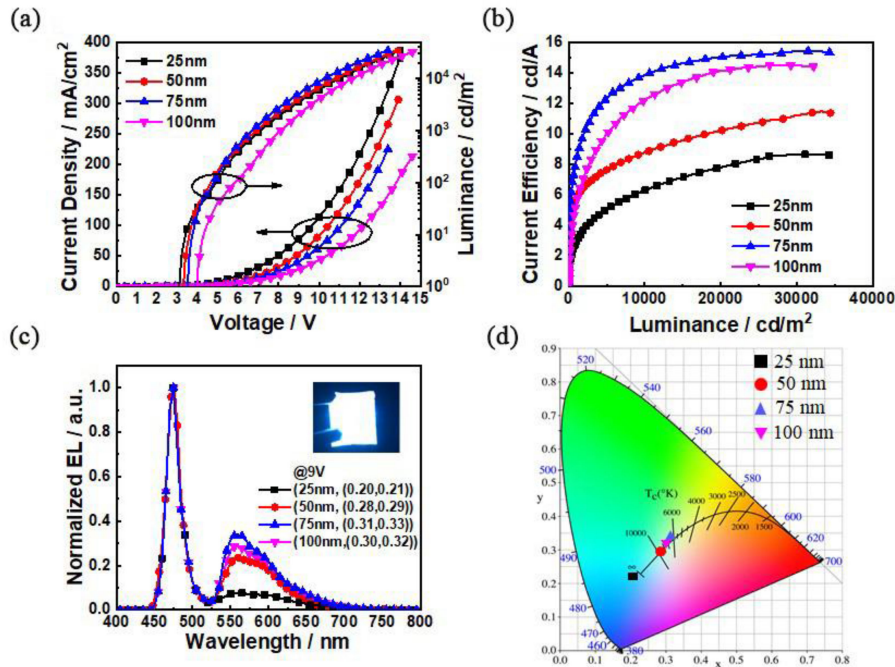
Fig. 2. (a) Current density-voltage-luminance (J-V-L), (b) current efficiency-luminance (CE-L), (c) EL spectra of the hybrid WLEDs with different thickness of Rubrene, where the inset shows an image of EL emission of the optimal device with 75 nm Rubrene at 9 V. (d) locations of the resulting hybrid WLEDs in the CIE 1931 chromaticity diagram.

of all devices are shown in Fig. 2. From the current density-voltage-luminance (J-V-L) characteristic of Fig. 2(a), it can be observed that all devices exhibit excellent rectifying diode characteristics. The lowest turn-on voltage is obtained to be 3.1 V, which is slightly higher than inorganic InGaN/GaN WLEDs. The highest luminance is achieved up to 35,000 cd/m^2, similar to the state-of-the-art white organic light emitting diodes [25], [26]. These results indicate that Rubrene and (InGaN/GaN) MQWs formed a good p-n junction. Fig. 2(c) shows the normalized EL spectra of the hybrid devices under the applied voltage of 9 V. As presented, the white emission is dominated by one main emission peak at 476 nm and two shoulders peak at 560 nm and 613 nm, which are assigned to the emissions from InGaN/GaN MQWs and Rubrene, respectively. The inset image in Fig. 2(c) is photograph of white-light emission from hybrid device under applied voltage of 9 V with excellent luminescence uniformity. Such results evidently revealed that Rubrene can sever as yellow-red emitting layer to produce white light as expected. Additionally, it is also noteworthy that the emission from Rubrene and the current efficiency increased first and then decreased as the thickness of Rubrene layer increased. When the thickness of the Rubrene is controlled to be 75 nm, the hybrid devices get the best performance. The optimal hybrid device presents a relatively low turn-on voltage of 3.5 V, a maximum current efficiency of 15.22 cd/A and a nearly purity white-light emission with CIE coordinates of (0.31, 0.33). The optimization of Rubrene thickness can not only enhance the hole injection but also balance the carrier recombination ratio between Rubrene and InGaN/GaN MQWs. With more carriers injected into LED, the captured and recombined carriers in Rubrene emitting layer change with its increasing thickness until the optimum balancing in carrier injection and transport is reached under certain applied bias.

However, Rubrene is deposited directly atop InGaN/GaN blue MQWs. Hence, there is a doubt whether the yellow-red emission originating from Rubrene layer is driven by photoluminescence (PL). To know exactly the luminescence mechanism of Rubrene in this hybrid WLED, the UV-vis absorption spectra of Rubrene were firstly investigated. The PL spectra of Rubrene film, InGaN/GaN MQWs as well as Rubrene (100 nm)/(InGaN/GaN) MQWs hybrid structure are shown in Fig. 3(a). For the Rubrene (100 nm)/(InGaN/GaN) MQWs hybrid structure, 476-nm blue light
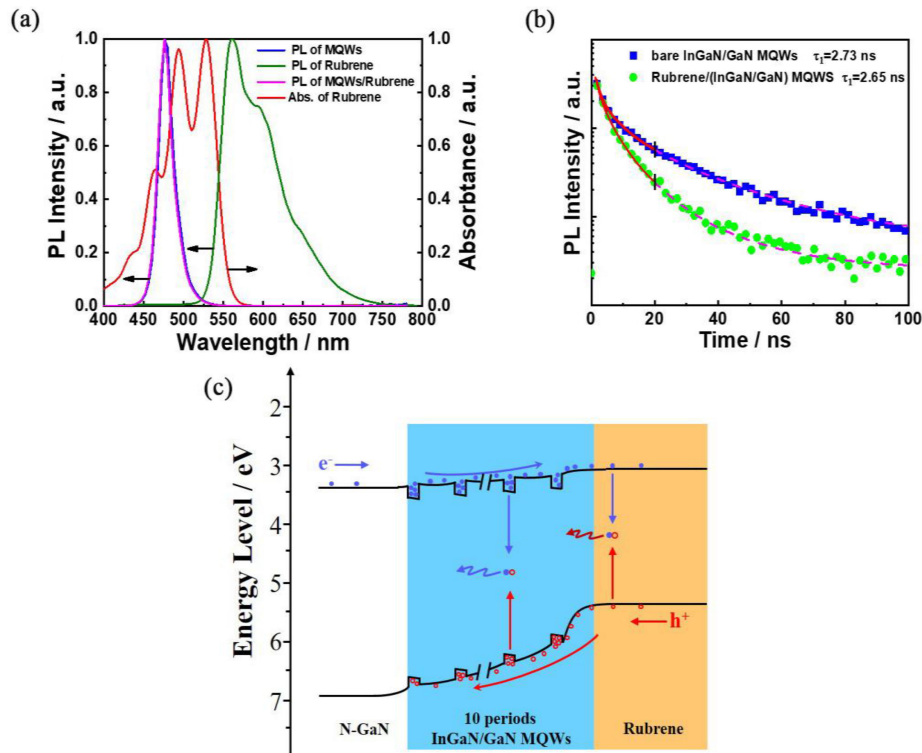
Fig. 3. (a) UV-visible absorption spectra of Rubrene, and PL spectra of Rubrene film, InGaN/GaN MQWs as well as Rubrene (100 nm)/(InGaN/GaN) MQWs structure using a 375 nm diode laser as an excitation source. (b) TRPL traces of the InGaN/GaN MQWs emission from the bare InGaN/GaN sample and the Rubrene/(InGaN/GaN) MQWs hybrid sample. (c) Carrier transport process across Rubrene/(InGaN/GaN) MQWs p-n junction under forward bias.

from the GaN/InGaN MQWs was used to photoexcite the single Rubrene layer. However, it was found in Fig. 3(a) that no obvious yellow-red emission from Rubrene in the PL spectra of Rubrene/(InGaN/GaN) MQWs hybrid structure compared to that shown in the EL spectra [see Fig. 2(c)]. Such huge difference confirms that the visible yellow-red light originates from the radiative recombination rather than color conversion. Additionally, it is widely known that light emission in LEDs originate from radiative recombination of carriers and energy transfer [27]. The spectra overlap [see Fig. 3(a)] between the PL spectrum of InGaN/GaN MQWs and absorption of Rubrene suggests the energy-transfer process from InGaN/GaN MQWs to Rubrene. To elucidate the carrier dynamics in Rubrene layer in hybrid WLED, the time-resolved photoluminescence (TRPL) measurements on InGaN/GaN MQWs in the hybrid WLED and the reference blue LED were performed. Fig. 3(b) demonstrates the TRPL decay traces of the two devices. A standard two exponential component model is used to study excitonic dynamics in MQWs, and thus TRPL traces [I(t)] can be described by [4], [15], [28]:

$$I(t) = a_1 \exp(-t/\tau_1) + a_2 \exp(-t/\tau_2) \tag{1}$$

where a_1 and a_2 are constants and τ_1 and τ_2 are the fast and slow components of the decay time of excitons in MQWs, respectively. At room temperature, both samples show $a_1 >> a_2$, meaning τ_1 can be taken as the representative fast-decay lifetime. The PL lifetime (τ_1) of the InGaN/GaN MQWs for the reference blue LED and the hybrid WLED are 2.73 ns and 2.65 ns, respectively. The slightly change of τ_1 should be attribute to the energy transfer between the Rubrene/MQWs. On one hand, Rubrene can absorbs the extra emitted light after pumping turns off. On the other hand, charge transfer excitons are likely to form at the Rubrene/MQWs interface, contributing to a long-wavelength emission. Both of these leads to a decrease in lifetime (τ_1). However, the Rubrene
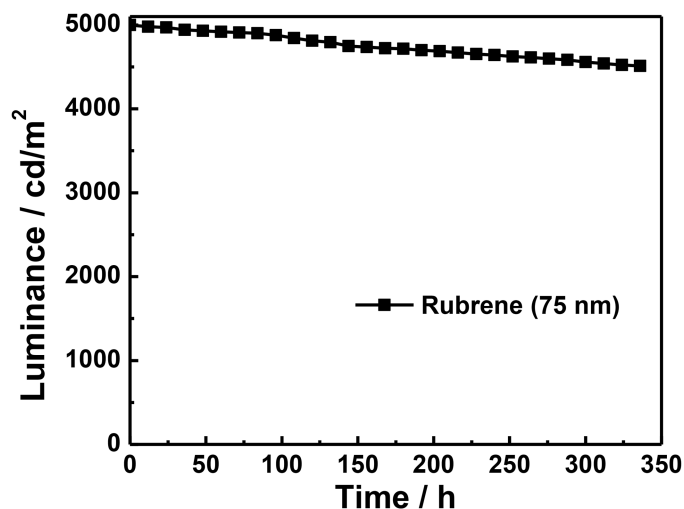
Fig. 4. Lifetime of the hybrid WLEDs with 75 nm Rubrene.

layer is very thin and only a small part of the light can be absorbed by it. Moreover, the charge transfer excitons have large radius and lower binding energy than Fenkel excitons [17]. Accordingly, the energy transfer between Rubrene and InGaN/GaN MQWs can be negligible. Thereafter, charge trapping followed by exciton formation in Rubrene layer is the dominant mechanism for yellow-red emission in hybrid WLEDs.

To further understand the carrier transport in Rubrene layer, the carrier transport mechanisms across the Rubrene/(InGaN/GaN) MQWs p-n junction interface were deeply analyzed. Fig. 3(c) illustrates the carrier transport process across Rubrene/(InGaN/GaN) MQWs p-n junction under applied forward bias. As mentioned before, the carrier mobility of Rubrene (up to 40 cm^2/Vs) is larger than the respective value of p-GaN (3.54 cm^2/Vs), which benefits more holes tunneling from Rubrene layer into InGaN/GaN MQWs. The injected holes and electrons would be confined in the quantum wells and recombine to emit blue light. On the other hand, owing to a small electron transport barrier (0.2 eV) between LUMO of Rubrene (3.2 eV) and conduction band of InGaN/GaN MQWs (3.4 eV), the excess electrons without recombination in InGaN/GaN MQWs can be easily transported to Rubrene layer. A portion of holes are accumulated in Rubrene side near the Rubrene/MQWs interface due to a relatively large $\triangle Ev$ between Rubrene and MQWs of 1.5 eV. The accumulated holes and the injected electrons would form Frenkel excitons by a strong Coulombic interaction. Then the Frenkel excitons recombine and radiate the yellow-red emission in the Rubrene layer. As the Rubrene layer increasing, the exciton formation region in Rubrene layer broadens and more excitons would form and recombine in Rubrene layer, thereby the yellow-red emission increases. It is important to balance the emission intensity of yellow-red light from the Rubrene layer and blue light from MQWs to achieve pure white light emission. When the Rubrene thickness exceeds a certain value, the holes accumulated in the Rubrene side of the Rubrene/MQWs interface will greatly increase. The accumulated holes will combine with electrons to form nonradiative recombination, resulting in exciton quenching. Eventually, the exciton quenching at the Rubrene/MQWs interface leads to the decreased device performance [29].

For white light luminescence, long-term stability is also one key factor for future commercialization, especially for hybrid organic/inorganic LEDs. The hybrid device with 75-nm-thick Rubrene layer was chosen to examine the device lifetime. It was strictly encapsulated before lifetime test in an air environment at a constant luminance of 5000 cd/m^2. As shown in Fig. 4, the luminance of hybrid LED only have 9% reduction after 15 days, which exhibits excellent long-term performance. Such good lifetime is attributed to the superior hole transport property of Rubrene leading to efficient and

balanced charge transport, which have been suggested to be the long device lifetime mechanism [30].

4. Conclusion

In summary, electrically driven hybrid organic/inorganic III-nitride WLEDs have been successfully achieved based on Rubrene/(InGaN/GaN) MQWs p-n junction. By studying the radiation and carrier transport of Rubrene and device performance, we found that Rubrene played an important role of yellow-red emitting layer and hole transporting layer owing to its excellent optical properties and high carrier mobility. After balancing the current flow, the optimized hybrid WLEDs have a nearly purity white light with color coordinates of (0.31, 0.33) and a maximum current efficacy of 15.22 cd/A. In addition, the hybrid WLEDs in this work have excellent long lifetime stability, which is promising for future commercialization. These results suggest that hybrid organic/inorganic WLEDs provide a promising route to fabricating multicolor micro-LED or large-area LEDs by constructing suitable hybrid organic/inorganic p-n junction.

Acknowledgment

References

[1] S. Reineke *et al.*, "White organic light-emitting diodes with fluorescent tube efficiency," *Nature*, vol. 459, pp. 234–238, 2009.
[2] X. Ye, F. Xiao, Y. X. Pan, Y. Y. Ma, and Q. Y. Zhang, "Phosphors in phosphor-converted white light-emitting diodes: Recent advances in materials, technique and properties," *Mater. Sci. Eng. R, Rep.*, vol. 71, pp. 1–34, 2010.
[3] M. X. Du *et al.*, "Novel emitting system based on a multifunctional bipolar phosphor: An effective approach for highly efficient warm-white light-emitting devices with high color-rendering index at high luminance," *Adv. Mater.*, vol. 28, pp. 5963–5968, 2016.
[4] Z. Zhuang *et al.*, "High color rendering index hybrid III-nitride/nanocrystals white light-emitting diodes," *Adv. Funct. Mater.*, vol. 26, pp. 36–43, 2016.
[5] S. H. Jeong, S. K. Oh, J. H. Ryou, K. S. Ahn, K. M. Song, and H. S. Kim, "Monolithic inorganic ZnO/GaN semiconductors heterojunction white light-emitting diodes," *ACS Appl. Mater. Interfaces*, vol. 10, pp. 3761–3768, 2018.
[6] S. Byeongchan *et al.*, "Improved carrier injection of AlGaN-based deep ultraviolet light emitting diodes with graded superlattice electron blocking layers," *RSC Adv.*, vol. 8, pp. 35528–35533, 2018.
[7] B. Damilano, N. Grandjean, C. Pernot, and J. Massies, "Monolitic white light emitting diodes based on InGaN/GaN multiple-quantum wells," *Jpn. J. Appl. Phys.*, vol. 40, pp. L918–L920, 2001.
[8] H. P. T. Nguyen *et al.*, "Controlling electron overflow in phosphor-free InGaN/GaN nanowire white light-emitting diodes," *Nano Lett.*, vol. 12, pp. 1317–1323, 2012.
[9] Y. J. Hong *et al.*, "Visible-color-tunable light-emitting diodes," *Adv. Mater.*, vol. 23, pp. 3284–3288, 2011.
[10] E. T. Shaw *et al.*, "Cool to warm white light emission from hybrid inorganic/organic light-emitting diodes," *J. Mater. Chem. C*, vol. 4, pp. 11499–11507, 2016.
[11] K. H. Kim and J. J. Kim, "Origin and control of orientation of phosphorescent and TADF dyes for high-efficiency OLEDs," *Adv. Mater.*, vol. 30, 2018, Art. no. 1705600.
[12] E. Hleli *et al.*, "Role of electron blocking layer in performance improvement of organic diodes," *J. Electron. Mater.*, vol. 48, pp. 3794–2800, 2019.
[13] K. W. Tsai, M. K. Hung, Y. H. Mao, and S. A. Chen, "Solution-processed thermally activated delayed fluorescent OLED with high EQE as 31% using high triplet energy crosslinkable hole transport materials," *Adv. Funct. Mater.*, vol. 29, 2019, Art. no. 190125.
[14] J. H. Na, M. Kitamura, M. Arita, and Y. Arakawa, "Dual luminescence from organic/inorganic hybrid p-n junction light-emitting diodes," *Appl. Phys. Lett.*, vol. 94, 2009, Art. no. 213302.
[15] S. Ghataora, R. M.Smith, M. Athanasiou, and T. Wang, "Electrically injected hybrid organic/inorganic III-nitride white light-emitting diodes with nonradiative Förster resonance energy transfer," *ACS Photon.*, vol. 5, pp. 642–647, 2018.
[16] S. R. Forrest, "Organic-on-inorganic semiconductor heterojunctions: Building block for the next generation of optoelectronic devices?," *IEEE Circuits Devices Mag.*, vol. 5, no. 3, pp. 33–37, Jun. 1989.
[17] Y. J. Wu, C. H. Liao, P. M. Lee, Y. S. Liu, C. L. Liu, and C. Y. Liu, "Organic/inorganic F8T2/GaN light emitting heterojunction," *Org. Electron.*, vol. 49, pp. 64–68, 2017.
[18] A. Kikuchi and T. Tsuji, "Electroluminescence characteristics of inorganic (p-GaN/MgO)-organic (Alq3) hybrid p-n junction light emitting diodes," in *Proc. Int. Conf. Mater. Res. Soc.*, 2011, vol. 1286, Art. no. e03-38.
[19] L. Q. Yang, X. X. Xu, and B. Wei, "Study on n-type GaN based organic-inorganic hybrid light emitting heterojunction," *J. Lumin.*, vol. 206, pp. 393–397, 2019.

[20] B. Liu *et al.*, "Al Incorporation, structural and optical properties of AlxGa1−xN (0.13 ≤ x ≤ 0.8) alloys grown by MOCVD," *J. Cryst. Growth*, vol. 310, pp. 4499–4502, 2008.

[21] T. Hasegawa and J. Takeya, "Organic field-effect transistors using single crystals," *Sci. Technol. Adv. Mater.*, vol. 10, pp. 024314–024329, 2009.

[22] H. Choukri, A. Fischer, S. Forget, S. Chénais, and M. C. Castex, "White organic light-emitting diodes with fine chromaticity tuning via ultrathin layer position shifting," *Appl. Phys. Lett.*, vol. 89, 2006, Art. no. 183513.

[23] A. K. Pandey and J. M. Nunzi, "Rubrene/fullerene heterostructures with a half-gap electroluminescence threshold and large photovoltage," *Adv. Mater.*, vol. 19, pp. 3613–3617, 2007.

[24] H. Kim *et al.*, "Nitride-organic semiconductor hybrid heterostructures for optoelectronic devices," *Physica Stat. Solidi C*, vol. 4, pp. 2411–2414, 2007.

[25] S. A. Ying *et al.*, "High efficiency color-tunable organic light-emitting diodes with ultra-thin emissive layers in blue phosphor doped exciplex," *Appl. Phys. Lett.*, vol. 114, 2019, Art. no. 033501.

[26] D. X. Luo *et al.*, "Extremely simplified, high-performance, and doping-free white organic light-emitting diodes based on a single thermally activated delayed fluorescent emitter," *ACS Energy Lett.*, vol. 3, pp. 1531–1538, 2018.

[27] Y. Q. Li, A. Rizzo, R. Cingolani, and G. Gigli, "Bright white-light-emitting device from ternary nanocrystal composites," *Adv. Mater.*, vol. 18, pp. 2545–2548, 2006.

[28] S. W. Feng *et al.*, "Two-component photoluminescence decay in InGaN/GaN multiple quantum well structures," *Physica Status Solidi (B)*, vol. 228, pp. 121–124, 2001.

[29] Z. B. Wang *et al.*, "Controlling carrier accumulation and exciton formation in organic light emitting diodes," *Appl. Phys. Lett.*, vol. 96, 2010, Art. no. 043303.

[30] R. Meerheim *et al.*, "Influence of charge balance and exciton distribution on efficiency and lifetime of phosphorescent organic light-emitting devices," *J. Appl. Phys.*, vol. 104, 2008, Art. no. 014510.